Extraction and Characterization of Cellulose Nanowhiskers from TEMPO Oxidized Sisal Fibers

FANGWEI FAN
Wuhan Textile University
MENGTING ZHU
Wuhan Textile University
KAIYANG FANG
Wuhan Textile University
ENDI CAO
DONGHULU SCHOOL
YINZHI YANG
Wuhan Textile University
JINPENG XIE
Wuhan Textile University
ZHONGMIN DENG
Wuhan Textile University
YIREN CHEN
Wuhan Textile University
XINWANG CAO (aswang1984@163.com)
wuhan textile university

Research Article

Keywords: Cellulose nanowhiskers, Sisal fibers, TEMPO-mediated oxidation, Alkali treatment, Homogenization

Posted Date: September 20th, 2021

DOI: https://doi.org/10.21203/rs.3.rs-805257/v1

Version of Record: A version of this preprint was published at Cellulose on November 11th, 2021. See the published version at https://doi.org/10.1007/s10570-021-04305-8.

Abstract

Cellulose nanowhiskers as one kind of renewable and biocompatible nanomaterials evoke much interest because of its versatility in various applications. Herein, the sisal cellulose nanowhiskers with length of 100–500 nm, ultrathin diameter of 6–61 nm, high crystallinity of 74.74 % and C6 carboxylate groups converted from C6 primary hydroxyls were prepared via a 2,2,6,6-tetramethylpiperidine-1-oxyl radical (TEMPO)/NaBr/NaClO system selective oxidization combined with mechanical homogenization. The effects of sodium hydroxide concentration in alkali pretreatment on the final sisal cellulose nanowhiskers were explored. It was found that with the increase of sodium hydroxide concentration, the sisal fiber crystalline type would change from cellulose I to cellulose II. The versatile sisal cellulose nanowhiskers would be particularly useful for applications in the nanocomposites as reinforcing phase, as well as in tissue engineering, filtration, pharmaceutical and optical industries as additives.

1. Introduction

A number of new nanomaterials with various excellent properties have been found and prepared in order to satisfy the development of social industry (Roduner 2006). Among them, due to increasingly serious environmental problems, nanocellulose with biocompatibility, renewable and sustainable properties have evoked particular attention and become an advanced raw material which has been widely investigated in the field of electronics (Nogi & Yano 2008), water filtration (Cao et al. 2013; Cao et al. 2020), medicine (Aziz et al. 2021), tissue engineering scaffolds (Luo et al. 2019; Ávila et al. 2015), sewage treatment (Ji et al. 2017), drug delivery materials (Müller et al. 2013), and etc.

Nanocellulose was firstly reported by Nickerson and Habrle (1947) in 1940s by strong acid hydrolysis, which has also become one of the most common methods until now. The greatest challenge encounted in this process was high energy consumption, besides, the effluent produced would be harmful to the environment and operational costs might increase regarding the necessity of intensive effluent treatments (Zain et al. 2014). In order to lower the energy consumption and protect the environment, different methods have been applied including biological method (Gupte et al. 2021), enzyme interaction (Cao and Tan 2004) and TEMPO-oxidation (Saito et al. 2007). Biological method mainly use the vital movement of some specific bacterias such as Acetobacter xylinum (Aryaie et al. 2019) to product nanocellulose, so this kind of cellulose is also called bacterial nanocellulose (BNC). Some bacterias could even use toxic compounds generated after industrial activities as carbon source to form cellulose (Marín et al. 2019). Enzymatic hydrolysis is another interesting pathway to produce nanocellulose (Karim et al. 2017), which mainly used the specificity of cellulase to hydrolyze the amorphous area in the fiber to prepare nanocellulose. In contrast, biological method and enzyme hydrolysis did not generate toxic residues as acid hydrolysis did, which were normally held in mild thermal and pressure conditions, resulting in a lower energy-intensive process (Fritz et al. 2015) but low efficiency.

In comparison, TEMPO oxidation method has the advantages of high efficiency, short time and simple operation. In addition, there are abundant sodium carboxylate groups on the fibril surfaces of cellulose,

enabling electrostatic repulsion and/or osmotic behavior to work effectively between the anionically charged TEMPO-treated nanofibrillated celluloses in water (Isogai et al. 2011; Poyraz et al. 2018). A number of applications have been involved with TEMPO oxidation nanocellulose. Saito et al. (2007) studied the oxidization of the -OH group at the C6 position of the pulp fiber to a charged carboxyl group to form a charge repulsion by TEMPO, and then prepared cellulose nanowhiskers (NC) through high-speed stirring. It not only had low energy consumption, but also prepared completely nanofibrillated wood fiber, which was of great significance to the development of cellulose. Yang et al. (2019) proposed a simple, effective and low-cost method ("coating" method), directly deposited micron-level 2,2,6,6-tetramethylpiperidine-1-oxyl (TEMPO) to oxidize wood fibers. The resulting film showed high total transmittance of 85 %,high haze of 62 %, a high tensile strength of 80 MPa and excellent thermal stability.

As a kind of typical non-wood fiber, sisal fibers is often used in lower end fields. The rational use of sisal can not only save forest resources and protect the environment, but also develop high value-added products. And because of its high cellulose content (47–48 %) (Martin et al. 2010) and high crystallinity, sisal fiber is actually very suitable as a raw material for preparing nanocellulose. To our knowledge, there was no researchers studying on the preparation of nanocellulose obtained from pretreated sisal leaf fiber by TEMPO oxidation combined with mechanical method.

Herein, the goal of the present work was to explore the structure and morphology of nanocellulose obtained from pretreated sisal leaf fiber by combination of TEMPO/NaBr/NaClO selection oxidation system and mechanical homogenization. The effects of different pretreatment conditions on sisal nanowhiskers were also explored. Finally, the samples were characterized by Fourier transform infrared (FTIR), X-ray diffraction (XRD), thermogravimetric analysis (TGA), scanning electron microscopy (SEM) and UV-vis spectrometer.

2. Experimental

2.1 Raw materials and chemicals

Sisal leaves were collected from sisal planting garden at Wuhan Textile University campus, after complete drying, the sisal leaves are torn into strips about 1 mm wide. The analytically pure sodium hydroxide (NaOH), hydrogen peroxide (H_2O_2), dimethylsulfoxide (DMSO), 2,2,6,6-tetramethylpiperidine-1-oxyl radical (TEMPO, 98%), sodium bromide (NaBr), sodium hypochlorite (NaClO, 12 wt%) solution, ethanol and other chemicals were of laboratory grade (Shanghai Aladdin Chemical Regent Inc., China) and used without further purification.

2.2 Degumming treatment of sisal fibers

In order to remove hemicellulose, pectin, lignin and other non-cellulose components in raw sisal fibers, and to improve the content of cellulose and utilization value of fiber, degummization of the fibers is necessary (Fan et al. 2010). Sisal fiber (20 g) were put in 3 wt% sodium hydroxide (NaOH) solution

(60mL) mixed with 2 wt% sodium silicate (Na_2SiO_3), then soaked in 90 ℃ water bath for 3 h. Then the fiber was washed to neutral with purified water and oven dried for 3 h at 60 ℃. In order to remove metal ions attached to the fibers, the dried fibers were put in a 3 % ethylenediaminetetraacetic acid (EDTA) solution under 30℃ water bath heating for 1 h, the ratio of material to liquid (w/w) was 1:40, then washed and oven dried. Then perform alkali oxygen treatment with the sodium hydroxide of 20 g/L, hydrogen peroxide of 22.5 mL/L, under 95 ℃ water bath heating for 3.5 h with ratio 1:50, then washed and oven dried for 24 h at 60 ℃ to obtain the degummed fiber.

2.3 Alkali treatment of degummed sisal fibers

The degummed sisal fiber was cut into 0.3 mm powder, and 5 g fiber was weighed after 60-mesh sample screening. The ground fibers were alkalized by NaOH solutions with selected concentrations of 5, 15 and 25 % at the temperature of 60 ℃ for 4 h, the ratio of material to liquid (w/w) was 1:50. After the alkalization processes, all the samples were sufficiently washed by deionize water several times and dried at 60 ℃ for 24 h. And then the fibers were placed in dimethyl sulfoxide solution with a ratio of 1:20, the fibers were heated in a water bath at 70 ℃ for 3 h. After the reaction, they were sufficiently washed and dried at 60 ℃ for 24 h for later use.

2.4 Preparation of sisal cellulose nanowhiskers

Preparation of cellulose nanowhiskers was performed according to the procedure described by (Cao et al. 2012). The alkali treated sisal fibers (1.0 g) were dispersed in deionized water (100 g). Then NaBr (0.20 g) and TEMPO (0.02 g) were both dissolved in the suspension and then stir at room temperature for 30 min. The reaction was started by the addition of 12 wt% NaClO solution (2 mL) under stirring. The PH was kept at 10 ~ 10.5 (Isogai et al., 2011) (Isogai et al. 2011), monitored with a PH meter, by adjusting with 1 wt% NaOH aqueous solution. The reaction was stopped by adding ethanol (5 mL) while no NaOH consumption, followed by continuously stirring for another 20 min. The final product was washed with deionized water by successive centrifugations (5000 rpm for 10 min) until neutral. The generated oxidized fiber cellulose slurry (1.0 g) was dispersed in 100 g of deionized water and sonicated for 10 min at 10,000 rpm with an IKA T25 homogenizer (IKA Works, Shanghai, China), and the recovered supernatant became the cellulose nanowhiskers aqueous suspension. The suspension was centrifuged at 5000 rpm for 10 min, and the supernatant was freeze-dried in a vacuum freeze dryer for 48 h to obtain sisal cellulose nanowhiskers.

2.5 Characterization

2.5.1 Optical transmittance of cellulose nanowhiskers suspension

Cellulose nanowhiskers suspension was introduced into a quartz cuvette, and the transmittance was measured from 200 to 900 nm using a UV-vis spectrometer (TU-1950, Beijing Instrument Ltd, China). The spectrum of a cuvette filled with water was used as a reference and to correct the transmittance of the suspension sample.

2.5.2 Scanning Electron Microscopy (SEM)

The surface morphologies of sisal fibers were observed using scanning electron microscope (JSM-6510 LV & JSM-7800F, JEOL, Japan). Prior to SEM evaluation, the samples were coated with a thin layer of gold by means of a plasma sputtering apparatus to avoid the charging effect. The SEM images was captured at different magnifications with an electron beam accelerating potential of 3 kV.

2.5.3 Fourier transform infrared (FTIR) spectroscopy

Infrared absorption spectroscopy is an important analysis method to study the relationship between infrared absorption and the molecular structure of substances. As one of the most mature analysis methods of polymer structure analysis, it is widely used in the research of fibers in the textile field. It was used to determine the chemical functional groups in sisal fibers and chemical changes in functional groups of fibers before and after treatment to evaluate the efficiency of each treatment. The powders of all samples were dispersed on KBr pellets and then performed on a Nicolet iS50, Thermo Fisher, USA. All the samples were recorded in the range of 4000 – 400 cm^{-1} region with 16 scans in each case at a resolution of 4 cm^{-1}.

2.5.4 X-ray diffraction (XRD) measurement

In order to investigate the crystallinity of untreated jute, alkali treated jute and jute cellulose nanowhiskers, the milled sample powders were analyzed at ambient temperature by step scanning on a X-ray diffractometer (PANalytical Empyrean, Panaco, Netherlands). The samples were scanned in the 2θ range of 10–45° and a scan rate of 8 °/min. The crystallinity index (CrI) of the material was calculated using the Eq. 1 (Ajouguim et al 2019; Achaby et al. 2018; Kassab et al. 2019) :

$$CrI(100\%)=(I_{200}-I_{am})/I_{200}\times100 \quad (1)$$

where CrI represents the relative degree of crystallinity, I_{200} is the maximum intensity of the (200) lattice diffraction at 2θ = 22.8°, and I_{am} is the intensity of diffraction at around 2θ = 18.6°.

2.5.5 Thermal gravimetric analysis (TGA)

Thermogravimetric analysis was employed to investigate the thermal stability of fibers before and after treatment. TG analysis of all the powdered samples was performed using a TG 209F1 Libra. Samples of approximately 5 mg were placed in a platinum crucible under nitrogen atmosphere with a heating rate of 10 ℃/min within the range of 30 to 600 ℃. TG curves show the variation of sample weight and derivative weight with temperature.

3. Results And Discussions

3.1 Crystalline structure

Figure 1 presented the X-ray diffraction patterns of sisal cellulose nanowhiskers prepared with different alkali concentrations and sisal fiber after different treatments. As we could see from Fig. 1 (a) when the alkali treatment concentration was 5 %, the X-ray diffraction peaks of the sisal cellulose nanowhiskers appeared at 2θ of 15°, 17°, 22.5° and 35°, which represented the (1–10), (110), (200) and (004) crystal faces of the cellulose, respectively. It showed typical cellulose structure. However, when the concentration of alkali treatment reaches 25 %, the X-ray diffraction peaks appeared at about 2θ of 12°, 20°, 22° and 35°, and the corresponding crystal faced of (1–10), (110), (020) and (004) of cellulose, respectively, showed typical cellulose structure. At the same time, it could be seen that when the alkali concentration was 15 %, the X-ray diffraction had both the characteristic peaks of cellulose type and , and the fiber at this time was a mixture of cellulose and , indicating that with the increase of the alkali concentration, the cellulose in sisal fiber would gradually transform from cellulose to cellulose , which was basically consistent with previous studies on this aspect (Yu et al. 2014).

Figure 1(b) showed the X-ray diffraction of degummed sisal fiber, 5 % alkali treated sisal fiber and TEMPO-oxidated sisal cellulose nanowhiskers, respectively. By comparing the X-ray diffraction patterns of sisal fiber before and after preparation, it could be seen that the preparation process of cellulose nanowhiskers had no effect on the basic crystal structure of cellulose. And as the noncellulose polysaccharides were removed and the amorphous zones were dissolved, the fibers showed increasing orientations along a particular axes. Calculated according to formula 1, the crystallinity thus went on increasing in going from the degummed sisal fiber (69.09 %) to 5% alkali-treated sisal fiber (69.97 %), and subsequently to oxidized sisal cellulose nanowhiskers (74.74 %). The little increasing in the crystallinity after TEMPO oxidization, which may be due to the increase of water solubility in the disordered area during centrifugal washing, resulting in partial loss (Saito and Isogai 2004).

3.2 FTIR analysis

Figure 2 showed the FT-IR spectra of sisal cellulose nanowhiskers prepared with different alkali concentrations and sisal fiber after different treatments. According to Fig. 2(a), the wide absorption peak of 3000–3500 cm^{-1} was generated by the stretching vibration of -OH bond, and there were two weak absorption peaks in sisal fiber treated with 5 % or 25 % alkali concentration. Zhang and Pan (1995) believed that the main reason was that there were two kinds of intramolecular hydrogen bonds in the fiber, and intermolecular hydrogen bonds were relatively complex. Meanwhile, when 5 % alkali was used to treat the fibers, the two absorption peaks were mainly at around 3250 cm^{-1}, while when the concentration reached 25 %, the two absorption peaks were shifted to around 3500 cm^{-1}, mainly because the cellulose adopted the anti-parallel chain mode, the polarity of the chain was low, and the perturbation to the free stretching vibration of -OH bond was small. 1365 cm^{-1} and 1315 cm^{-1} respectively represented the bending vibration of -CH and the swinging motion of $-CH_2$. With the increase of treatment concentration intensity, the strength changed, mainly due to the different hydrogen bonding environment of $-CH_2$ and -OH in cellulose due to the change of crystalline form of cellulose. The absorption peak at 1110 cm^{-1} was caused by the C-O stretching vibration of the cellulose six-membered ring framework, and the absorption peak was nearly disappeared with the increase of alkali

concentration, which was related to the change of hydrogen bond. Another significant difference was that the absorption peak near 895 cm^{-1} gradually increases with the increase of alkali concentration, which was caused by the different skeleton vibration of C_1 atom. The changes of the five characteristic peaks above all indicated that with the increase of alkali concentration, the crystal form of sisal fiber gradually changed from cellulose Ⅰ to cellulose Ⅱ, which was consistent with the X-ray diffraction analysis results of the sisal fiber above.

Figure 2 (b) showed that the basic peak shape of sisal fiber changed little before and after preparation, only some specific groups changed, and most groups only changed in strength. The main changes of the peaks at 1607 cm^{-1} and 1415 cm^{-1} were mainly caused by the vibration of the C = O bond of the carboxyl group formed by the oxidation of the primary alcohol hydroxyl group of the cellulose by the TEMPO-oxidation system, indicated that hydroxyl groups at the C_6 position of cellulose molecules are converted to sodium carboxylate (Fukuzumi et al. 2009). The wide absorption peak near 3300 cm^{-1} represented the stretching vibration of OH bond. The change of the absorption peak indicated that after the preparation and treatment of nano-cellulose, the content of cellulose was getting higher and higher. At the same time, the oxidation process of TEMPO-oxidation system was a selective oxidation process, which only acted on the primary alcohol hydroxyl group of cellulose.

3.3 Thermal performance

Figure 3 showed the TG diagrams of sisal cellulose nanowhiskers prepared with different alkali concentrations, TG and DTG diagrams of sisal fibers after different treatments. As could be seen from Fig. 3(a), the thermal stability of sisal nanowhiskers prepared with different sodium hydroxide concentrations was basically not significantly different, but the initial decomposition temperature of the fibers also changed a little due to the change of the crystalline form of the cellulose. With the increase of the concentration of alkali treatment, the initial decomposition temperature of the fiber would decrease, mainly because the thermal stability of cellulose Ⅰ was worse than that of cellulose Ⅱ, and the increase of the alkali concentration would make the crystal form of the cellulose transform from the cellulose amorphous type to the cellulose solid type, which was consistent with the results of the X-ray diffraction and infrared analysis.

As shown in Fig. 3 (b) and (c), all TG curves, showed a small amount of weight loss between 30 ℃ and 150 ℃, which was mainly due to the reduction of the water chemisorbed on the surface of the fiber or the water attached by hydrogen bonds between fiber molecules. After the alkali treatment, the initial decomposition temperature of sisal fiber was significantly increased, which indicated that the non-cellulose components which were not completely removed in the previous degumming treatment were removed in the alkali treatment process, and the residual mass of the final alkali treatment sisal fiber was less than that after the degumming treatment, which also indicated this. After alkali treatment, the sisal fiber began to thermally degrade at 300°C, while the degradation temperature of TEMPO-oxidized sisal cellulose nanowhiskers started at 220°C. This indicated that the primary alcohol hydroxyl groups on the cellulose surface were caused by TEMPO oxidation. Oxidation into carboxyl groups would significantly

reduce the thermal degradation point of cellulose (Fukuzumi et al. 2010), which was basically in line with the results of previous studies.

It was worth noting that the DTG curve of TEMPO-oxidized sisal cellulose nanowhiskers was very broad, and it could be seen that the degradation process of sisal cellulose nanowhiskers was mainly composed of two decomposition stages. The former was due to the thermal degradation point of the sodium anhydroglucuronate unit, while the latter was significantly lower than that of unoxidized sisal fiber, indicating the present of more thermally unstable anhydroglucuronate units in the TEMPO-oxidized sisal fibers, and the crystalline cellulose chain in the DTG peak reduced (Cao et al. 2012).

3.4 Micro-structure

Figure 4 showed the SEM micrographs of the degummed sisal fiber, alkali treated sisal fiber and TEMPO-oxidated sisal cellulose nanowhiskers and the width distribution of nanowhiskers. As seen from Fig. 4 (a) and (b), the degummed sisal fiber was a filament with a diameter of 10–20 μm, while the sisal fiber that was crushed and screened and then treated with sodium hydroxide and DMSO became thinner and shorter, with a diameter of about 10 μm, and length between 0.1–0.3 mm, this was due to the alkali treatment acted on the fibers could contribute to remove hemi-cellulose, surface impurities, and a part of lignin from the fibers (Meng et al. 2016), as well as the inter-molecular hydrogen bonding, leading to the decrease of fiber diameter, also DMSO was a kind of strong hydrogen bonding-breaking agent, treatment further contributed to the breakage of inter-molecular hydrogen bonding and dissolution of interior and external non-cellulose materials, resulting in a further dimensional diminution of the sisal fibers (Das et al. 2010; Lin et al. 2014). Figure 4 (c) showed that after TEMPO oxidation reaction combined with high-speed homogenization, most of the fibrils were prepared into nano-sized fiber whiskers. These cellulose nanowhiksers were rod-shaped, with a width of 6–61 nm (Fig. 4 (d)) and a length of 100–500 nm. At the same time, it could be seen that some nanowhiskers gather together, which was mainly caused by the high specific surface area of cellulose nanowhiskers and the large number of strong hydrogen bonded between the fibers.

3.5 Optical transmittance of nanowhiskers suspension

Figure 5 showed the UV-vis transmittance of 0.1 wt% cellulose nanowhiskers suspension and the digital photographs of the suspensions of the obtained nanowhiskers in a beaker. The transmittance of the 0.1 wt% cellulose nanowhiskers suspension at 900 nm was approximately 90 %, which is consistent with the experimental results in our previous work (Cao et al. 2012). TEMPO oxidation system treated sisal fibers could introduce carboxylates along the surface of the whiskers and result in a negative-charged surface (Lin et al. 2014). Therefore, the stability of transparent suspensions could be interpreted by the anionic stabilization via the attraction/repulsion forces of electrical double layers (Liu et al. 2015; Kargarzadeh et al. 2012).

4. Conclusions

In this study, a stable and transparent dispersion of sisal cellulose nanowhiskers with a widthof 6-60 nm were prepared from chemically pretreated sisal fibers by TEMPO selectively oxidizedtreatment combined with mechanical homogenization. At the same time, the effect of alkali treatment concentration in the pretreatment stage on the performance of preparing cellulose nanowhiskers was analyzed, and it was found that as the concentration of sodium hydroxide increased, sisal fiberscrystalline type would gradually change from cellulose I tocellulose □.When the alkali concentration was 5%, the sisal fiber appeared as cellulosel. When the alkali concentration was 15%, the sisal fiber appeared as a mixture of cellulose I and□,and the concentration was increased to 25%, it was expressed as cellulose □. The preparation of such tunable polymorphic cellulose nanowhiskers will enable cellulose nanowhiskers to exhibit more expected properties, thereby expanding its application fields. The in-depth development and utilization of sisal fiber will not only increase the added value of sisal products, but also protect the environment and resources.

5. Declarations

Acknowledgement

This work was supported by National Natural Science Foundation of China Youth Fund (51503162); general project of Hubei Provincial Natural Science Foundation (2016cfb459); national innovation training program for college students (201910495014); technical innovation program of Hubei Province (2019aaa005); innovation training program for university students of Hubei Province (s201910495063).

Conflict of interest

We declare that we have no financial and personal relationships with other people or organizations that can inappropriately influence our work, there is no professional or other personal interest of any nature or kind in any product, service and/or company that could be construed as influencing the position presented in, or the review of the manuscript entitled.

Human and animal rights

This manuscript did not contain any animal studies or human participants involvement in the study, which also complies with ethical approval and ethical standards.

6. References

1. Achaby ME, Miri NE, Hannache H, et al (2018) Cellulose nanocrystals from Miscanthus fibers: insights into rheological, physicochemical properties and polymer reinforcing ability. Cellulose25:6603- 6619
2. Ajouguim S, Abdelouahdi K, Waqif M, et al (2019) Modifications of Alfa fibers by alkali and hydrothermal treatment. Cellulose 26(3):1503-1516

3. Aryaie MMH, Zeydanloo S, Dehghani FAMR, et al(2019) Producing and evaluating of Bacterial Nano-cellulose (BNC) using Acetobacter xylinum bacterial. Journal of Wood and Forest Science and Technology 26(3):29-42
4. Ávila HM, Feldmann EM, Pleumeekers MM, et al (2015) Novel bilayer bacterial cellulose nanowhiskers scaffold supports neocartilage formation in vitro and in vivo. Biomaterials 44: 122-133
5. Aziz T, Ullah A, Fan H, et al (2021) Cellulose nanocrystals applications in health, medicine and catalysis. J Polym Environment 29(4):1-10.
6. Cao X, Ding B, Yu J, et al(2012) Cellulose nanowhiskers extracted from TEMPO-oxidized jute fibers. Carbohyd Polym 90(2): 1075-1080
7. Cao X, Huang M, Ding B, Yu J, Sun G(2013) Robust polyacrylonitrile nanofibrous membrane reinforced with jute cellulose nanowhiskers for water purification, Desalination 316: 120-126
8. Cao X, Zhu M, Fan F, et al (2020) All-cellulose composites based on jute cellulose nanowhiskers and electrospun cellulose acetate (CA) fibrous membranes. Cellulose 27, 1385-1391
9. Cao Y, Tan H (2004) Structural characterization of cellulose with enzymatic treatment. J Mol Struc 705(1-3): 189-193
10. Das K, Ray D, Banerjee C, et al (2010) Physicomechanical and thermal properties of jute-nanofiber-reinforced biocopolyester composites. Ind EngChem Res 49(6): 2775-2782.
11. Fan XS, Liu ZW, Liu ZT, et al(2010) A novel chemical degumming process for ramie bast fiber. Text Res J 80(19): 2046-2051
12. Fukuzumi H, Saito T, Iwata T, et al(2009) Transparent and high gas barrier films of cellulose nanofibers prepared by TEMPO-mediated oxidation. Biomacromolecules10(1): 162-165
13. Fukuzumi H, Saito T, Okita Y, et al (2010) Thermal stabilization of TEMPO-oxidized cellulose. Polym Degrad Stab 95(9): 1502-1508
14. Fritz C, Jeuck B, Salas C, et al(2015) Nanocellulose and proteins: exploiting their interactions for production, immobilization, and synthesis of biocompatible materials. Cellulose chemistry and properties: fibers, cellulose nanocellulose and advanced materials 207-224
15. Gupte Y, Kulkarni A, Raut B, et al(2021) Characterization of nanocellulose production by strains of Komagataeibacter sp. isolated from organic waste and Kombucha. Carbohyd Polym 266, 118176
16. Isogai A, Saito T, Fukuzumi H(2011) TEMPO-oxidized cellulose nanofibers. Nanoscale 3(1): 71-85
17. Ji YL, Kim EH, Park TU, et al (2017) Development of metal ion absorbing filter using cellulose nanofibrils. Palpu Chongi Gisul/Journal of Korea Technical Associationof the Pulp and Paper Industry 49(3):95-101
18. Kargarzadeh H, Ahmad I, Abdullah I, et al (2012) Effects of hydrolysis conditions on the morphology, crystallinity, and thermal stability of cellulose nanocrystals extracted from kenaf bast fibers. Cellulose 19(3): 855-866
19. Karim Z, Afrin S, Husain Q, et al(2017) Necessity of enzymatic hydrolysis for production and functionalization of nanocelluloses. Crit Rev Biotechnol37(3): 355-370.

20. Kassab Z, Boujemaoui A, Youcef HB, et al (2019) Production of cellulose nanofibrils from alfa fibers and its nanoreinforcement potential in polymer nanocomposites. Cellulose 26(18): 9567-9581
21. Liu DY, Sui GX, Bhattacharyya D (2015) Properties and characterization of electrically conductive nanocellulose-based composite films, Fillers and Reinforcements for Advanced Nanocomposites. Woodhead Publishing, 3-25
22. Liu H, Geng S, Hu P, et al (2015) Study of pickering emulsion stabilized by sulfonated cellulose nanowhiskers extracted from sisal fiber. Colloid Polym Sci293,963-974
23. Lin J, Yu L, Tian F, et al (2014) Cellulose nanofibrils aerogels generated from jute fibers. Carbohyd Polym 109: 35-43
24. Luo H, Cha R, Li J, et al(2019) Advances in tissue engineering of cellulose nanowhiskers-based scaffolds: a review. Carbohyd Polym 224: 115144
25. Marín P, MartiraniVASM, Urbina L, et al (2019) Bacterial cellulose nanowhiskers production from naphthalene. Microb Biotechnol 12(4):662-676
26. Martin AR, Martins MA, Silva ORF, Mattoso LHC(2010) Studies on the thermal properties of sisal fiber and its constituents. Thermochimi Acta 506(s1-2): 14-19
27. Meng C, Liu F, Li Z, Yu C (2016) The cellulose protection agent used in the oxidation degumming of ramie. Text Res J 86(10): 1109-1118
28. Müller A, Ni Z, Hessler N, et al (2013) The biopolymer bacterial cellulose nanowhiskers as drug delivery system: investigation of drug loading and release using the model protein albumin. J Pharm Sci 102(2): 579-592
29. Nickerson RF, Habrle JA (1947) Cellulose intercrystalline structure. Ind Eng Chem 39(11): 1507-1512
30. Nogi M, Yano H (2008) Transparent nanocomposites based on cellulose produced by bacteria offer potential innovation in the electronics device industry. Adv Mater20(10): 1849-1852
31. Poyraz B, Tozluoğlu A, Candan Z, et al(2018) TEMPO-treated CNF composites: pulp and matrix effect. Fibers Polym, 19(1): 195-204
32. Roduner E (2006) Size matters: why nanomaterials are different. Chem Soc Rev 35(7): 583-592.
33. Saito T, Isogai A (2004) TEMPO-mediated oxidation of native cellulose. The effect of oxidation conditions on chemical and crystal structures of the water-insoluble fractions. Biomacromolecules 5(5): 1983-1989
34. Saito T, Kimura S, Nishiyama Y, et al (2007) Cellulose nanofibers prepared by TEMPO-mediated oxidation of native cellulose. Biomacromolecules 8(8): 2485-2491
35. Yang W, Jiao L, Liu W, et al (2019) Manufacture of highly transparent and hazy cellulose nanofibril films via coating TEMPO-oxidized wood fibers. Nanomaterials 9(1): 107
36. Yu L, Lin J, Tian F, et al (2014) Cellulose nanofibrils generated from jute fibers with tunable polymorphs and crystallinity. J Mat Chem A, 2(18): 6402-6411
37. Zain NFM, Yusop SM, Ahmad I(2014) Preparation and characterization of cellulose and nanocellulose from pomelo (Citrus grandis) albedo. J Nutri Food Sci 5(1), 334.

38. Zhang J, Pan HS (1995) The FTIR Study of Microcrystalline Cellulose. Cell Sci Technol 3(1):22-27

Figures

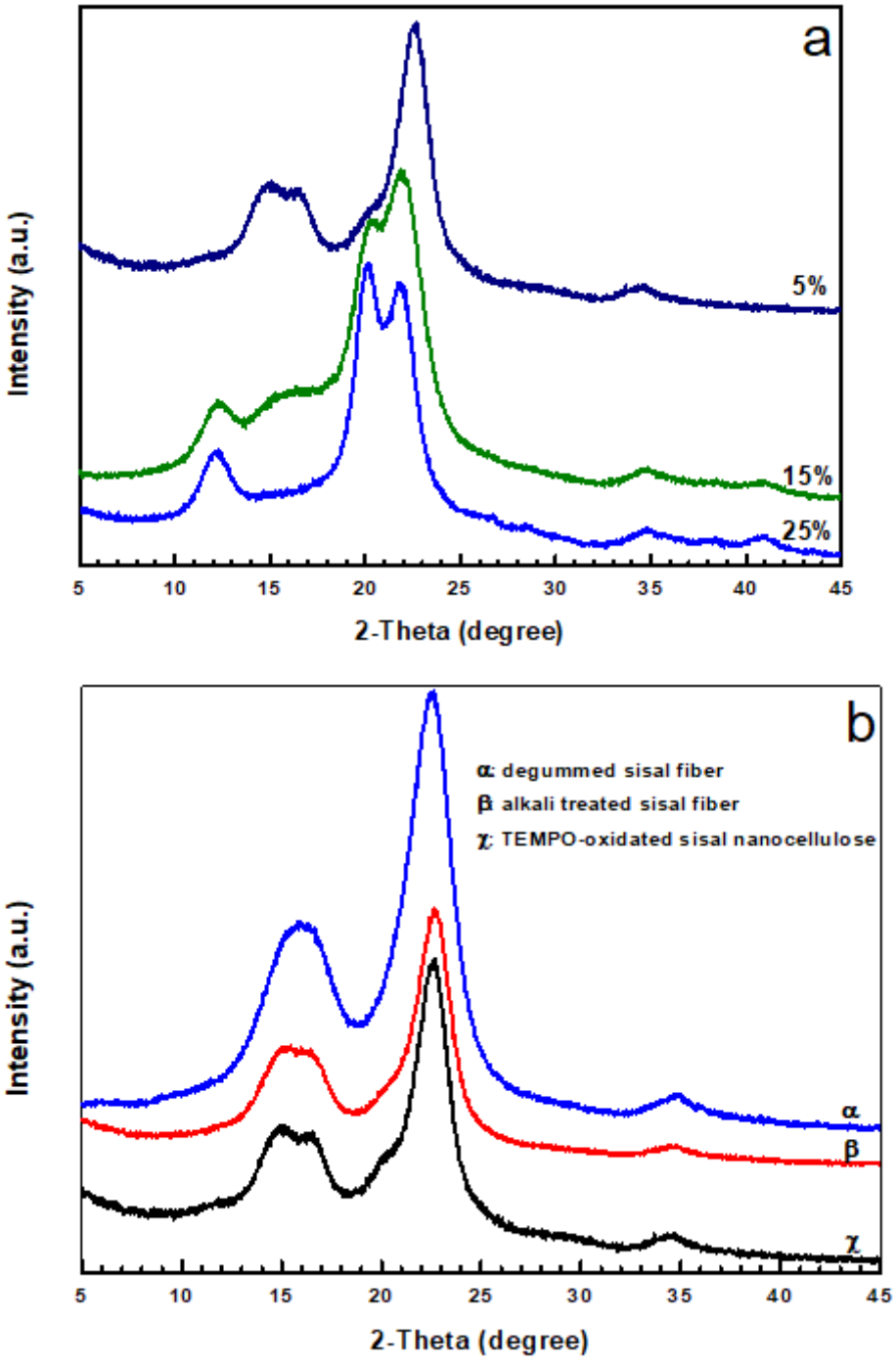

Figure 1

X-ray diffraction patterns of (a) sisal cellulose nanowhiskers prepared with different alkali concentrations; and (b) sisal fibersafter differenttreatments.

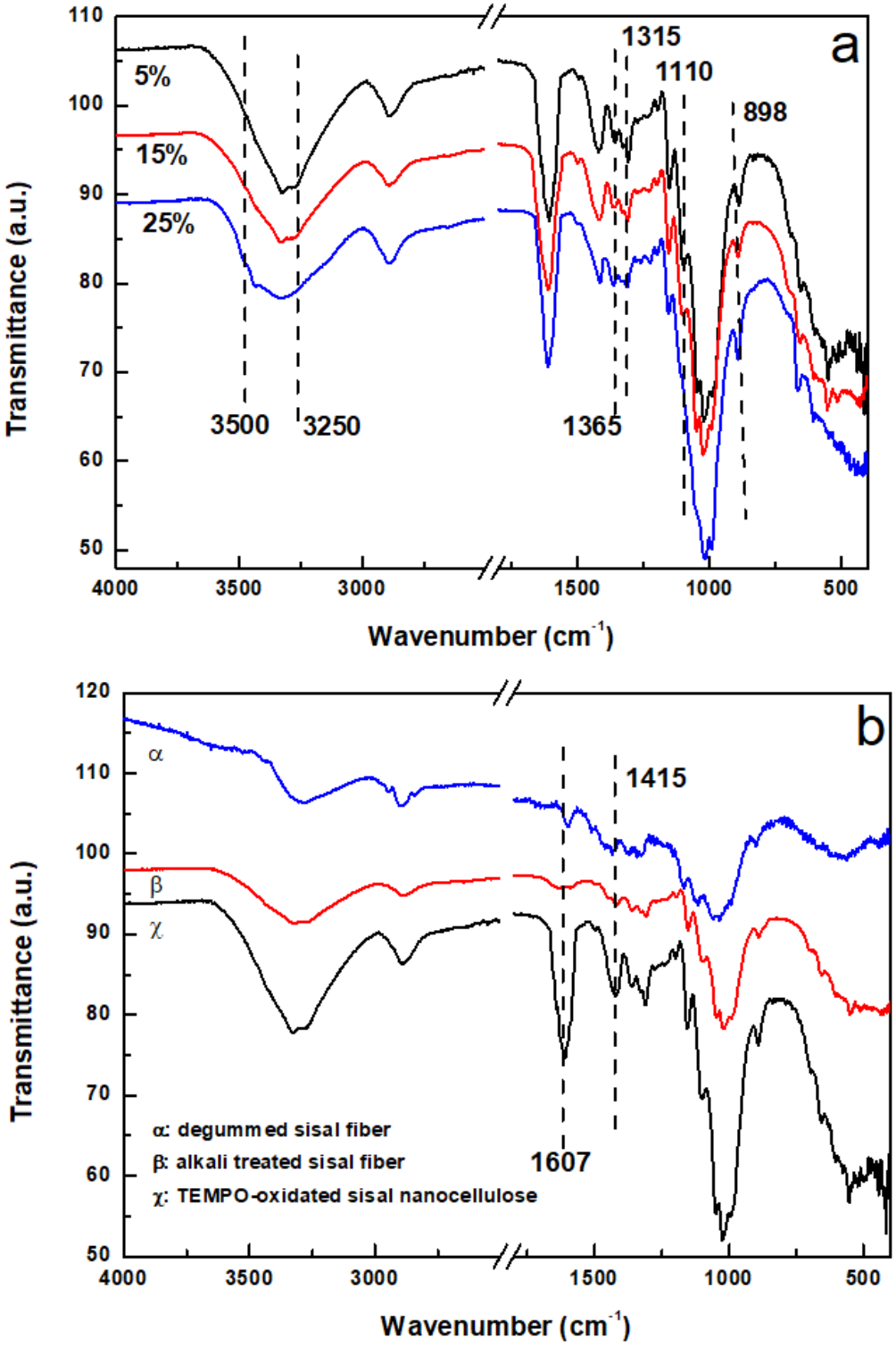

Figure 2

FT-IR spectra of (a) sisal cellulose nanowhiskers prepared with different alkali concentrations; (b) sisal fibers after different treatments.

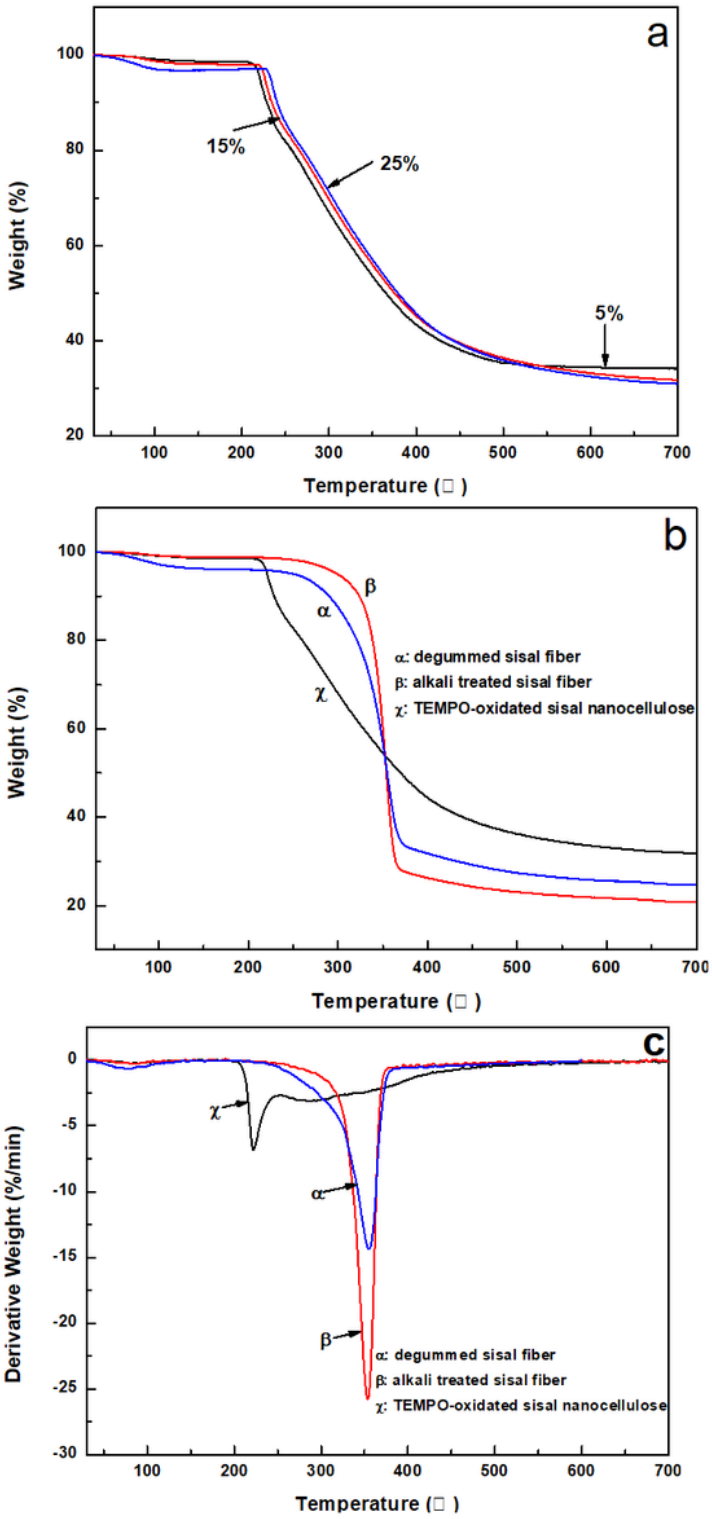

Figure 3

(a) TG diagrams of sisal cellulose nanowhiskersprepared with different alkali concentrations; (b) TG and (c) DTG diagrams of sisal fibersafter different treatments.

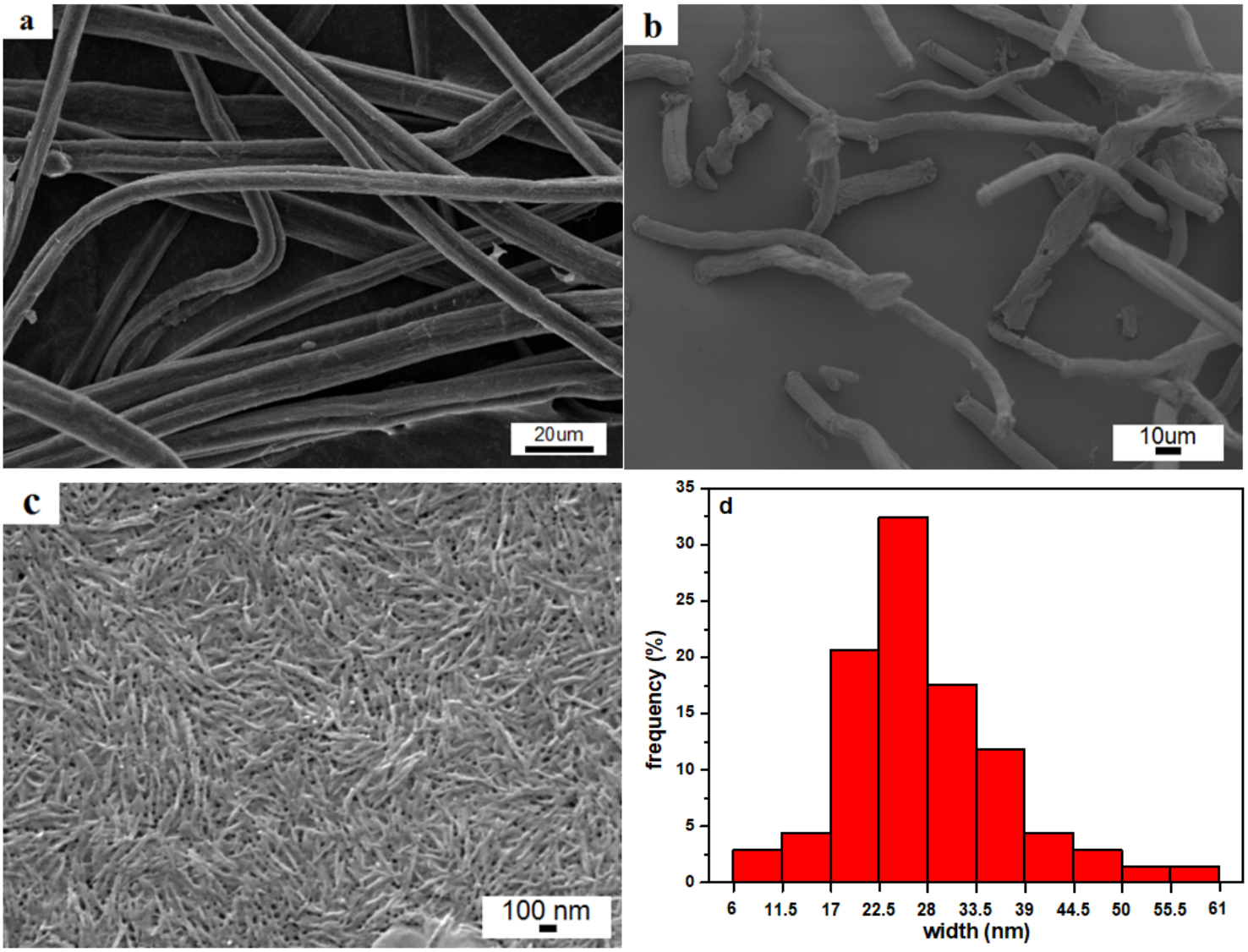

Figure 4

SEM micrographs of (a) degummed sisal fiber; (b) alkali treated sisal fiber;(c) TEMPO-oxidated sisal cellulose nanowhiskers. and (d) width distribution of cellulose nanowhiskers.

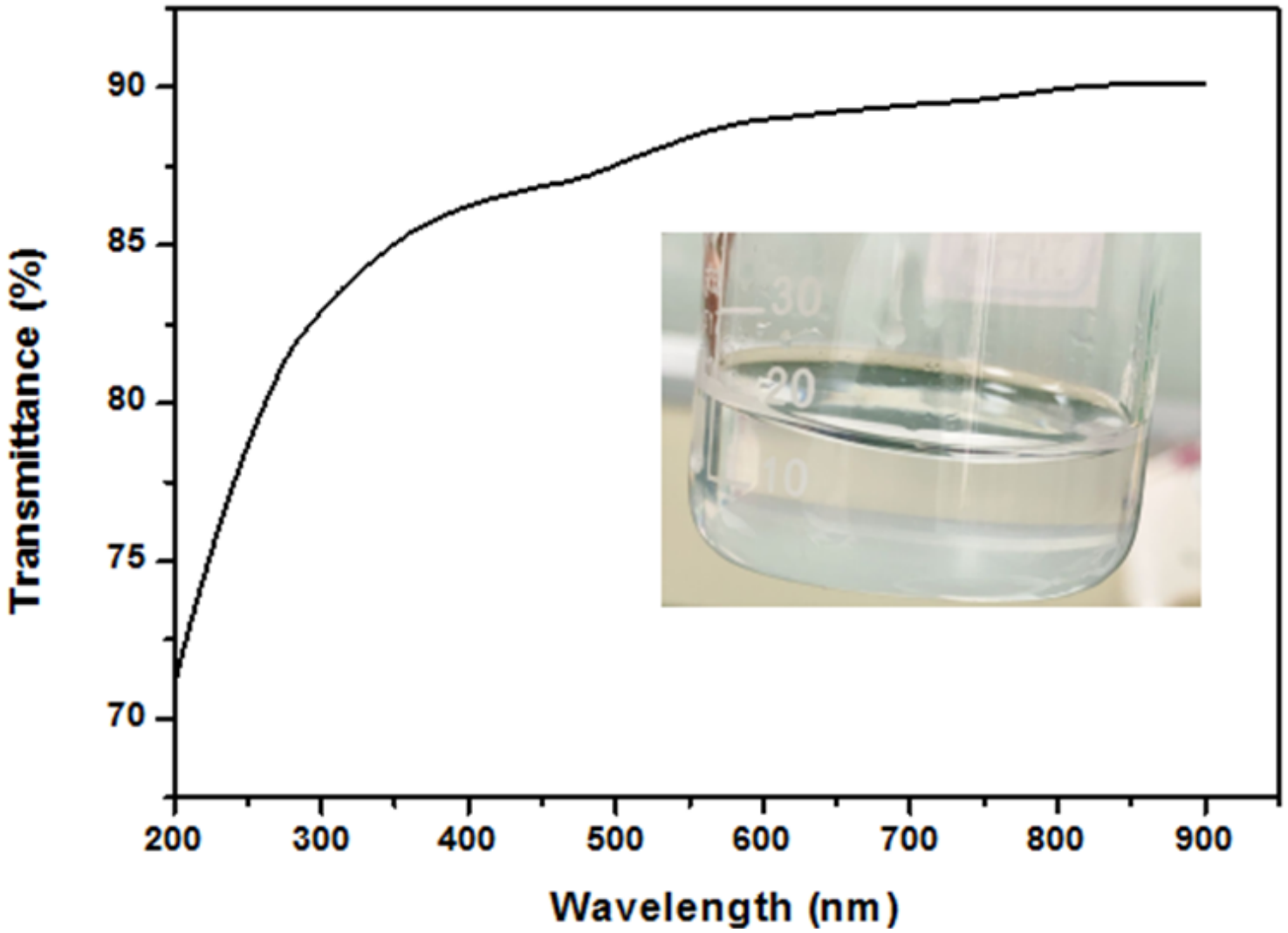

Figure 5

UV-vis transmittance of 0.1 wt% cellulose nanowhiskers suspension prepared from TEMPO-oxidized sisal fibers. The inset photograph shows light transmittance behavior of the cellulose nanowhiskers suspension.